Preprints, 18th IFAC Workshop on Control Applications of Optimization
July 18-22, 2022. Gif sur Yvette, France

Nonlinearity handling in MPC for Power Congestion management in sub-transmission areas

Thanh-Hung Pham * **Alessio Iovine** * **Sorin Olaru** *
Jean Maeght ** **Patrick Panciatici** ** **Manuel Ruiz** **

* *Laboratory of Signals and Systems (L2S), CNRS, CentraleSupélec, Paris-Saclay University, Gif-sur-Yvette, France*
{firstname.lastname}@centralesupelec.fr
** *Réseau de Transport d'Électricité (RTE), Paris, France*
{firstname.lastname}@rte-france.com

Abstract: This paper proposes congestion management solutions based on Model Predictive Control (MPC) principles for transmission network zones. The contribution resides in the use of logical variables for describing the nonlinearities related to the modelling of the physical aspects in power curtailment, or some desired control goals. This allows for the representation of the nonlinear model of a sub-transmission zone with a storage device in a linear Mixed Logical Dynamical (MLD) formulation, then paving the way to the utilisation of linear mixed integer programming for the optimization problem. Moreover, part of the contribution considers supplementary temporal specifications for the energy storage device utilisation. This is modelled using additional temporal and logical variables as part of the system state and control signal. Consequently, the extended model of the power network zone is formulated as a linear MLD system and integrated to the MPC design. The proposed controllers are validated through simulations on an industrial case-study.

1. INTRODUCTION

Due to the need to integrate renewable power, the power congestion management problem for electrical networks is increasing in complexity (Meyer et al. (2020)). Indeed, the raising presence of renewable power multiplies the situations where the power production exceeds the maximum allowed power on the transmission lines. If this excess is not admissible in design specifications, the lines with power congestion problems during the operation may be disconnected from the network, which possibly leads to a cascading lines opening or blackouts (Monforti-Ferrario and Blanco (2021)). One of the innovative approaches employed by Transmission System Operators (TSOs) to manage congestion and reduce their impact on the lines is related to the utilisation of energy storage devices and renewable power curtailment through model-based optimization. As a consequence, approaches based on Model Predictive Control (MPC) can be used to design congestion management algorithms(see Hoang et al. (2021)).

When considering renewable power curtailment, the resulting models are nonlinear. In Iovine et al. (2021), the authors propose a linear approximated model where the variation of the produced power is described as a disturbance pre-estimated based on forecasted available power without the curtailment action. Though the control design using this model efficiently works in a specific scenario as described in Hoang et al. (2021), the exact nonlinearity of the network zone is not taken into account in the MPC prediction mechanism, and is shown to affect the effectiveness of the proposed control system. In the present paper, we target to investigate the use of Mixed Logical Dynamical (MLD) formalism (see Bemporad and Morari (1999)) in order to handle nonlinearities and obtain a not too computational demanding Mixed Integer Linear Programming (MILP).

Moreover, we focus on the problem that the storage energy device is used for multiple tasks and by different users; therefore, a sharing agreement is required. In Straub et al. (2019), the bounds of the battery power and energy are scheduled for a day based on hourly forecasted grid states to avoid the congestion in the zone. In Perez et al. (2016), the sharing policy is formulated such that the economical benefit from batteries is maximized via predefined pricing rules for different services. However, in some situations when the TSO is not the battery owner or the congestion management is not prioritized, the battery availability duration is strictly limited, and thus, supplementary temporal specifications must be considered. For a self-consistent MPC design, additional temporal and logical variables are investigated in our work as part of the state and control signals that determine the battery power limitations. The adopted approach represents the extended system using the MLD formulation which results in a MILP for the MPC optimization problem. To investigate pros and cons

⋆ This work was carried out within the CPS4EU project, which has received funding from the ECSEL Joint Undertaking (JU) under grant agreement No 826276. The JU receives support from the European Union's Horizon 2020 research and innovation program and France, Spain, Hungary, Italy, Germany. The proposed results reflect only the authors' view. The JU is not responsible for any use that may be made of the information the present work contains.

of the possibility to consider a reduction of the number of binary variables, we avoid the formalism of Signal Temporal Logic (see Raman et al. (2014)), that usually implies the utilisation of tools which automatically generate the needed binary variables and are not customizable.

As contributions, we consider two modelling frameworks. In the first model, the nonlinear dynamics of the renewable power generator with partial curtailment are considered in a linear MLD formulation. In the second model, the nonlinear zone dynamics and supplementary temporal specifications of battery availability for the congestion management are represented using the linear MLD formalism. For the presented models, we propose and solve receding horizon optimal control problems based on MPC via MILP.

Notations: $\mathcal{Z}^N$ is the set of nodes in the considered zone. $\mathcal{Z}^C$ is the set of nodes where the curtailment of the generated power is allowed. $\mathcal{Z}^B$ is the set of nodes with a battery. $\mathcal{Z}^L$ is the set of power lines in the zone. n^N, n^C, n^B, n^L are their cardinalities.

2. CONGESTION MANAGEMENT VIA MPC

2.1 Linear MLD modelling for zonal power networks

Let the state variables include the power flow $F_j(t)$ of line j, the curtailment of the renewable power $P_n^C(t)$ at node n, the battery power output $P_m^B(t)$ at node m, the battery energy $E_m^B(t)$ at node m, the available renewable power $P_n^A(t)$ at node n and the produced power $P_n^P(t)$ at node n. The control inputs are the power variations of $P_n^C(t)$ and $P_m^B(t)$, i.e., $\Delta P_n^C(t)$ and $\Delta P_m^B(t)$. The variation $\Delta P_n^A(t)$ of the available power represents a disturbance inside of the zone while $\Delta P_l^T(t)$ describes the unknown power variation disturbance at node l due to power flow outside of the zone. The nonlinear dynamical equations of the zone model are, $\forall (j,n,m,l) \in \mathcal{Z}^L \times \mathcal{Z}^C \times \mathcal{Z}^B \times \mathcal{Z}^N$ (Iovine et al. (2021)):

$$\begin{cases} F_j(t+1) = F_j(t) + \sum_{m\in\mathcal{Z}^B} b_j^m \Delta P_m^B(t-d) + \\ \qquad \sum_{n\in\mathcal{Z}^C} b_j^n \Delta P_n^P(t) + \sum_{l\in\mathcal{Z}^N} b_j^l \Delta P_l^T(t), \\ P_n^C(t+1) = P_n^C(t) + \Delta P_n^C(t-\tau), \\ P_m^B(t+1) = P_m^B(t) + \Delta P_m^B(t-d), \\ E_m^B(t+1) = E_m^B(t) - Tc_m^B[P_m^B(t) + \Delta P_m^B(t-d)], \\ P_n^P(t+1) = P_n^P(t) + \Delta P_n^P(t), \\ P_n^A(t+1) = P_n^A(t) + \Delta P_n^A(t), \\ P_n^P(t+1) = \min\left(P_n^A(t+1), \overline{P}_n^P - P_n^C(t+1)\right), \end{cases} \tag{1}$$

where $b_j^{m/n/l}$ are constant parameters based on the concept of Power Transfer Distribution Factor (PTDF) (see Cheng and Overbye (2005)), c_m^B is constant power reduction factor for the batteries, $\overline{P}_n^P > 0$ is the maximum power that can be produced by the renewable generator n, T is the sampling time, d and τ are the operational time delays of the control actions for the battery power output and the generator power curtailment, respectively, with $\tau \geq d \geq 1$. The state and control variables respect the following constraints, $\forall (j,n,m,l) \in \mathcal{Z}^L \times \mathcal{Z}^C \times \mathcal{Z}^B \times \mathcal{Z}^N$:

$$-L_j \leq F_j(t) \leq L_j, \quad 0 \leq P_n^C(t) \leq \bar{P}_n^P, \tag{2a}$$
$$\underline{P}_m^B \leq P_m^B(t) \leq \bar{P}_m^B, \tag{2b}$$
$$\underline{E}_m^B \leq E_m^B(t) \leq \bar{E}_m^B, \quad 0 \leq \Delta P_n^C(t) \leq \bar{P}_n^P, \tag{2c}$$
$$\underline{P}_m^B - \bar{P}_m^B \leq \Delta P_m^B(t) \leq \bar{P}_m^B - \underline{P}_m^B, \tag{2d}$$

with the upper and lower bounds $L_j > 0$, $\overline{P}_n^P > 0$, $\underline{P}_m^B < 0$, $\overline{P}_m^B > 0$, $\underline{E}_m^B > 0$, and $\overline{E}_m^B > 0$.

In (1), the non-linearity resides in the implicit equation describing the produced renewable power evolution $P_n^P(t)$. As the first contribution of the present work, this is represented in a linear MLD form as presented in the following. Let the logical variable $\delta_n^P(t) \in \{0,1\}$ and the real variable $z_n^P(t) \in \mathbb{R}_+$, $\forall\, n \in \mathcal{Z}^C$, be defined as:

$$\begin{cases} \left[\delta_n^P(t) = 1\right] \Leftrightarrow \left[P_n^A(t) + \Delta P_n^A(t) \right. \\ \qquad\qquad \left. \leq \overline{P}_n^P - P_n^C(t) - \Delta P_n^C(t-\tau)\right], \\ z_n^P(t) = \min\left(P_n^A(t) + \Delta P_n^A(t), \right. \\ \qquad\qquad \left. \overline{P}_n^P - P_n^C(t) - \Delta P_n^C(t-\tau)\right). \end{cases} \tag{3}$$

Hence, the system dynamics (1) is rewritten as:

$$\begin{cases} F_j(t+1) = F_j(t) + \sum_{m\in\mathcal{Z}^B} b_j^m \Delta P_m^B(t-d) + \\ \qquad \sum_{n\in\mathcal{Z}^C} b_j^n \left[z_n^P(t) - P_n^P(t)\right] + \sum_{l\in\mathcal{Z}^N} b_j^l \Delta P_l^T(t), \\ P_n^C(t+1) = P_n^C(t) + \Delta P_n^C(t-\tau), \\ P_m^B(t+1) = P_m^B(t) + \Delta P_m^B(t-d), \\ E_m^B(t+1) = E_m^B(t) - Tc_m^B[P_m^B(t) + \Delta P_m^B(t-d)], \\ P_n^P(t+1) = z_n^P(t), \\ P_n^A(t+1) = P_n^A(t) + \Delta P_n^A(t). \end{cases} \tag{4}$$

Using big-M formulation, $\delta_n^P(t)$ and $z_n^P(t)$ defined in (3) are embedded in the solution of the following system of linear inequalities:

$$\begin{cases} -M\delta_n^P(t) + \gamma \leq P_n^A(t) + \Delta P_n^A(t) - \overline{P}_n^P + P_n^C(t) \\ \qquad\qquad + \Delta P_n^C(t-\tau) \leq M\left(1 - \delta_n^P(t)\right), \\ z_n^P(t) \leq P_n^A(t) + \Delta P_n^A(t), \\ z_n^P(t) \geq P_n^A(t) + \Delta P_n^A(t) - M\left(1 - \delta_n^P(t)\right), \\ z_n^P(t) \leq \overline{P}_n^P - P_n^C(t) - \Delta P_n^C(t-\tau), \\ z_n^P(t) \geq \overline{P}_n^P - P_n^C(t) - \Delta P_n^C(t-\tau) - M\delta_n^P(t), \end{cases} \tag{5}$$

where $M \in \mathbb{R}_+$ is a sufficiently large scalar, and $\gamma \in \mathbb{R}_+$ is a small scalar. Notice that (4) is a standard explicit linear MLD system, where $\delta_n^P(t)$ and $z_n^P(t)$ are determined from the state and control variables at the instant t through inequality constraints (5). Then, the state variables at the next instant $t+1$ are computed from the state and control variables, δ_n^P and z_n^P at the previous instant t through an explicit formula. However, for a numerically efficient implementation, a compact mathematical model, where $P_n^A(t)+\Delta P_n^A(t)$, $P_n^C(t)+\Delta P_n^C(t-\tau)$ and $z_n^P(t)$ in (4) - (5) are replaced by $P_n^A(t+1)$, $P_n^C(t+1)$ and $P_n^P(t+1)$, can be employed without changing the solvability and uniqueness of the zonal network model.

To describe the model in a compact form, we define, $\forall j \in \mathcal{Z}^L$, $\forall\, n \in \mathcal{Z}^C$, $\forall m \in \mathcal{Z}^B$, $\forall l \in \mathcal{Z}^N$:

$$F(t) = col[F_j(t)],\ \Delta P^T(t) = col[\Delta P_l^T(t)], \tag{6a}$$
$$P^C(t) = col[P_n^C(t)],\ \Delta P^C(t) = col[\Delta P_n^C(t)], \tag{6b}$$
$$P^B(t) = col[P_m^B(t)],\ \Delta P^B(t) = col[\Delta P_m^B(t)], \tag{6c}$$
$$E^B(t) = col[E_m^B(t)], \tag{6d}$$
$$P^A(t) = col[P_n^A(t)],\ \Delta P^A(t) = col[\Delta P_n^A(t)], \tag{6e}$$

$$P^P(t) = col[P_n^P(t)],\ \Delta P^P(t) = col[\Delta P_n^P(t)], \quad (6f)$$
$$\delta^P(t) = col[\delta_n^P(t)],\ z^P(t) = col[z_n^P(t)], \quad (6g)$$
$$\overline{L} = col[L_j],\ \overline{P}^P = col[\overline{P}_n^P],\ \underline{P}^B = col[\underline{P}_m^B], \quad (6h)$$
$$\overline{P}^B = col[\overline{P}_m^B],\ \underline{E}^B = col[\underline{E}_m^B],\ \overline{E}^B = col[\overline{E}_m^B]. \quad (6i)$$

To deal with the known actuator delays, the system state disturbance and control vectors are defined as $x(t) = [F(t)\ P^C(t)\ P^B(t)\ E^B(t)\ P^P(t)\ P^A(t)\ \Delta P^C(t-\tau)\ \dots\ \Delta P^C(t-1)\ \Delta P^B(t-d)\ \dots\ \Delta P^B(t-1)]^\top \in \mathbb{R}^{n^L+(3+\tau)n^C+(2+d)n^B}$, $w(t) = [\Delta P^T(t)\ \Delta P^A(t)]^\top \in \mathbb{R}^{n^N+n^C}$, $u(t) = [\Delta P^C(t)\ \Delta P^B(t)]^\top \in \mathbb{R}^{n^C+n^B}$, respectively. Consequently, the resulting not-delayed system dynamics derived from (4)-(5) are:

$$\begin{cases} x(t+1) = \tilde{A}x(t) + \tilde{B}u(t) + \tilde{B}_z z^P(t) + \tilde{D}w(t), \\ a^P \geq \tilde{C}_x x(t) + C_z z^P(t) + C_\delta \delta^P(t) + C_w w(t), \end{cases} \quad (7)$$

where the matrices $\tilde{A}$, $\tilde{B}$, $\tilde{B}_z$, $\tilde{D}$, $\tilde{C}_x$, C_z, C_δ, C_w and a^P are suitable matrices. The system model (7) is used for the control design in the next subsection.

2.2 Control design

Fig. 1 illustrates the control strategy, that is composed by *Estimation* and *MPC* blocks. In the sequel of the paper, the prediction horizon is N. Moreover, the predicted or estimated value of $g(.)$ at the sampling $t+k$ given the available information at the sampling t is denoted as $g(k|t)$.

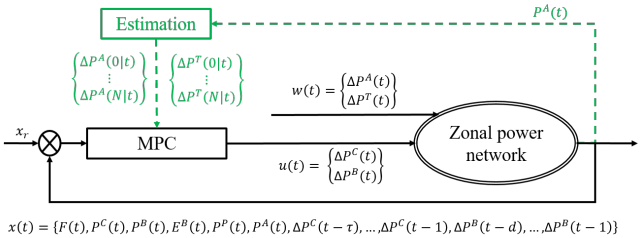

Fig. 1. Control scheme.

The *Estimation* block predicts the variation of the available generator power $\Delta P^A(k|t)$ and the external interaction $\Delta P^T(k|t)$ over the prediction horizon gathered in the disturbance $w(k|t)$. For robustness, the profile of $\Delta P^A(k|t)$ is considered to be constant $\forall\ k \in [0, \dots, N-1]$. In the same vein, there are multiple approaches for the prediction of $\Delta P^T(k|t)$. These choices can be integrated easily in the present control design. The performance of the disturbance estimation is not in the scope of the present work, and thus we will consider the simple one such as $\Delta P^T(k|t) = \mathbf{0}$.

The *MPC* block determines the control signals $u(t)$ using the predicted disturbance sequences $w(k|t)$ and the state feedback $x(t)$. Different from Hoang et al. (2021), this work directly takes into account the estimation of $\Delta P^A(k|t)$ in the MPC formalism via $w(k|t)$ without a supplementary prediction of $\Delta P^P(k|t)$ thanks to the consideration of the nonlinear model (1). To ensure the control problem feasibility, soft constraints are imposed to the flow on the power lines $F(k|t)$ for $k \in [d+1, \tau]$ using the softening slack variables $\varepsilon(k|t) \in \mathbb{R}^{n^L}$ such as $\varepsilon(k|t) > 0$, $\forall k \in [d+1, \tau]$, and $\varepsilon(k|t) = 0$, otherwise. Therefore, from (2) and (6), the constraints for the state $x(t)$ and for the control signal $u(t)$ are rewritten as:

$$x_{min}(k|t) \leq Cx(k|t) \leq x_{max}(k|t),\ \forall k \in [d+1, N], \quad (8a)$$
$$u_{min} \leq u(k|t) \leq u_{max},\ \forall k \in [0, N-1], \quad (8b)$$

where $C = [\mathbf{I}_{n^L+n^C+2n^B} \quad \mathbf{0}]$, and

$$x_{\min}(k|t) = [-\overline{L} - \varepsilon(k|t) \quad \mathbf{0} \quad \underline{P}^B \quad \underline{E}^B]^\top, \quad (9a)$$
$$x_{\max}(k|t) = [\ \overline{L} + \varepsilon(k|t) \quad \overline{P}^P \quad \overline{P}^B \quad \overline{E}^B]^\top, \quad (9b)$$
$$u_{min} = [\mathbf{0} \qquad \underline{P}^B - \overline{P}^B]^\top, \quad (9c)$$
$$u_{max} = [\overline{P}^P \qquad \overline{P}^B - \underline{P}^B]^\top. \quad (9d)$$

A cost function considering actuator delays is defined as:

$$J(t) = \sum_{k=1}^{N} \Big[\|x(k|t) - x_r\|_Q^2 + \|u(k-1|t)\|_R^2 + \|\varepsilon(k|t)\|_\beta^2 \Big], \quad (10)$$

where Q and R are positive semi-definite matrices; β is a positive scalar; x_r is the state reference. Thus, the MPC optimization problem is defined as:

$$\begin{aligned} \mathcal{O}_1 = \underset{\{u(0|t),\dots,u(N-1|t)\}}{\text{argmin}} \quad & J(t) \text{ in (10)} \\ s.t.\ & (7)\ \forall k \in [0, N-1],\ (8a)\ \forall k \in [d+1, N], \\ & (8b)\ \forall k \in [0, N-1],\ (9). \end{aligned} \quad (11)$$

The structure of this receding horizon optimization builds on the minimization of a convex cost, while the constraints are related to the dynamics and the input-state limitations, adequately enforced according to the delay in the actuation. Moreover, the implementation of the optimisation problem (11) includes $(n^L+(4+\tau)n^C+(3+d)n^B)N + n^L(\tau-d)$ real and $n^C N$ binary variables. Then, the first control actions $\Delta P^C(0|t)$ and $\Delta P^B(0|t)$ will be applied to the power networks at the instants $t+\tau$ and $t+d$, respectively.

3. BATTERY MANAGEMENT VIA MPC

The previously described control design supposes that the battery is completely dedicated to the congestion management operated by the TSO. However, in many situations, the battery exploitation is supposed to be used for a different task, mainly related to energy market participation, and TSOs are allowed to request to adapt the power output to grid's necessity only in few cases, as for example pro tempore congestion management. In the subsequent developments, we consider the above mentioned case, and therefore suppose that in normal conditions the battery power output will track a reference value P_m^{Br}, $\forall m \in \mathcal{Z}^B$, and that the TSO is allowed to take control over the battery power output only if needed, and to impose a different power output only for a short period of time. As a consequence, two following operation modes are defined for the battery power output:

- Unavailability mode: it must track the reference value P_m^{Br} for at least a given duration T_{off}^B;
- Availability mode: it is allowed to track a different value for a given duration T_{on}^B, which covers the delay period τ of renewable power curtailment, i.e., $\tau \leq T_{on}^B$.

In this section, a MLD model describing the previous specifications is introduced, thus allowing to consider

realistic time constraints on the possibility for the TSO to use the battery for power congestion management. The modelling is composed by two temporal variables as part of the system state and one logical variable as control signal. For a linear and explicit model formulation, four supplementary auxiliary variables are considered. These variables are then integrated in the MPC design.

3.1 Battery power specifications

For the battery at the bus m^{th}, the logical variable $\delta_m^u(t) \in \{0,1\}$ is defined such that $\delta_m^u(t) = 1$ if the battery is available, and $\delta_m^u(t) = 0$ otherwise. Hence, the constraints (2b) of battery power are reformulated as:

$$\begin{cases} P_m^B(t+1) \leq P_m^{Br} + \left(\bar{P}_m^B - P_m^{Br}\right)\delta_m^u(t), \\ P_m^B(t+1) \geq P_m^{Br} + \left(\underline{P}_m^B - P_m^{Br}\right)\delta_m^u(t). \end{cases} \tag{12}$$

To represents the durations of Availability and Unavailability modes, we define the temporal variables $t_m^{on}(t), t_m^{off}(t) \in \mathbb{N}$ such as:

$$\begin{cases} t_m^{on}(t+1) = \left[t_m^{on}(t)+1\right]\delta_m^u(t), \\ t_m^{off}(t+1) = \left[t_m^{off}(t)+1\right]\left(1-\delta_m^u(t)\right), \end{cases} \tag{13}$$

where $t_m^{on}(0) = 0$ and $t_m^{off}(0) = 0$. The additional control signal $\delta_m^u(t)$ respect the following implications:

$$\begin{cases} 1 \leq t_m^{on}(t) \leq T_{on}^B - 1 \Rightarrow \delta_m^u(t) = 1, \\ t_m^{on}(t) \geq T_{on}^B \Rightarrow \delta_m^u(t) = 0, \\ 1 \leq t_m^{off}(t) \leq T_{off}^B - 1 \Rightarrow \delta_m^u(t) = 0. \end{cases} \tag{14}$$

Let the real variable $z_m^{on}(t), z_m^{off}(t) \in \mathbb{R}_+$ and the logical variables $\delta_m^{on}(t), \delta_m^{off}(t) \in \{0,1\}$ be defined as:

$$\begin{cases} z_m^{on}(t) = \left[t_m^{on}(t)+1\right]\delta_m^u(t), \\ z_m^{off}(t) = \left[t_m^{off}(t)+1\right]\left(1-\delta_m^u(t)\right), \\ \delta_m^{on/off}(t) = 1 \Leftrightarrow \left[t_m^{on/off}(t) \geq 1\right]. \end{cases} \tag{15}$$

Equation (15) implies that the unique values of $z_m^{on/off}(t)$ and $\delta_m^{on/off}(t)$ are determined from given values of state $t_m^{on/off}(t)$ and control signal $\delta_m^u(t)$. Using big-M formulation, we replace the nonlinear relations in (15) by the following linear inequalities:

$$\begin{cases} -M_1\left(1-\delta_m^u(t)\right) \leq z_m^{on}(t) - t_m^{on}(t) - 1 \leq M_1\left(1-\delta_m^u(t)\right), \\ -M_1\delta_m^u(t) \leq z_m^{on}(t) \leq M_1\delta_m^u(t), \\ -M_1\delta_m^u(t) \leq z_m^{off}(t) - t_m^{off}(t) - 1 \leq M_1\delta_m^u(t), \\ -M_1\left(1-\delta_m^u(t)\right) \leq z_m^{off}(t) \leq M_1\left(1-\delta_m^u(t)\right), \\ -M_1\left(1-\delta_m^{on}(t)\right) \leq t_m^{on}(t) - 1 \leq \left(M_1+\gamma\right)\delta_m^{on}(t) - \gamma, \\ -M_1\left(1-\delta_m^{off}(t)\right) \leq t_m^{off}(t) - 1 \leq \left(M_1+\gamma\right)\delta_m^{off}(t) - \gamma, \end{cases} \tag{16}$$

where $M_1 \in \mathbb{R}_+$ is a sufficiently large scalar, and $\gamma \in \mathbb{R}_+$ is a small value. The utilization of $z_m^{on/off}(t)$ in (15) allows us to rewrite the nonlinear dynamics of the temporal variables (13) in a linear form:

$$t_m^{on/off}(t+1) = z_m^{on/off}(t). \tag{17}$$

Notice that the battery temporal specifications are mathematically represented in (14) by logical statements where the switching of battery operation modes described by $\delta_m^u(t)$ respects constraints on the mode durations described by $t_m^{on/off}(t)$. Thanks to big-M formulation, the battery specifications (14) are equivalent to:

$$\begin{aligned} t_m^{on}(t) - T_{on}^B + 1 + M_2\left(1-\delta_m^{on}(t)\right) \\ \geq \gamma - \left(M_3+\gamma\right)\delta_m^u(t), \end{aligned} \tag{18a}$$

$$t_m^{off}(t) - T_{off}^B + 1 + M_2\left(1-\delta_m^{off}(t)\right) \geq \gamma - \left(M_3+\gamma\right)\left(1-\delta_m^u(t)\right), \tag{18b}$$

$$-t_m^{on}(t) + T_{on}^B \geq \gamma - \left(M_3+\gamma\right)\left(1-\delta_m^u(t)\right), \tag{18c}$$

where $M_2, M_3 \in \mathbb{R}_+$ are sufficiently large scalars, and $\gamma \in \mathbb{R}_+$ is a sufficiently small scalar, both allowing to bound the binary relaxations. For numerical implementation, $z_m^{on}(t)$ and $z_m^{off}(t)$ in (16) and (18) can be replaced by $t_m^{on}(t+1)$ and $t_m^{off}(t+1)$ without changing the solvability and uniqueness of the additional dynamics. Let the vectors $t^B(t)$, $\delta^B(t)$, $z^B(t)$ and $\delta^u(t)$ be defined as:

$$\begin{cases} t^B(t) = \left[col\left[t_m^{on}(t)\right]^\top \quad col\left[t_m^{off}(t)\right]^\top\right]^\top, \\ \delta^B(t) = \left[col\left[\delta_m^{on}(t)\right]^\top \quad col\left[\delta_m^{off}(t)\right]^\top\right]^\top, \\ z^B(t) = \left[col\left[z_m^{on}(t)\right]^\top \quad col\left[z_m^{off}(t)\right]^\top\right]^\top, \\ \delta^u(t) = col\left[\delta_m^u(t)\right]. \end{cases} \tag{19}$$

Hence, we rewrite (16)-(18) in a compact form:

$$\begin{cases} t^B(t+1) = z^B(t), \\ a^B \geq C_x^B t^B(t) + C_u^B \delta^u(t) + C_\delta^B \delta^B(t) + C_z^B z^B(t), \\ a^t \geq C_x^t t^B(t) + C_u^t \delta^u(t) + C_\delta^t \delta^B(t), \end{cases} \tag{20}$$

where $a^t \in \mathbb{R}^{3n^B}$, $C_x^t \in \mathbb{R}^{3n^B \times 2n^B}$, $C_u^t \in \mathbb{R}^{3n^B \times n^B}$, $C_\delta^t \in \mathbb{R}^{3n^B \times 2n^B}$, $a^B \in \mathbb{R}^{12n^B}$, $C_u^B \in \mathbb{R}^{12n^B \times n^B}$, C_x^B, C_δ^B, $C_z^B \in \mathbb{R}^{12n^B \times 2n^B}$ are suitable matrices. By combining (7) and (20), an extended system can be defined, where the state, the control and the auxiliary variables are $\hat{x}(t) = \left[x(t)\ t^B(t)\right]^\top \in \mathbb{R}^{n^L+(3+\tau)n^C+(4+d)n^B}$, $\hat{u}(t) = \left[u(t)\ \delta^u(t)\right]^\top \in \mathbb{R}^{n^C+2n^B}$, $\hat{\delta}(t) = \left[\delta^P(t)\ \delta^B(t)\right]^\top \in \mathbb{R}^{n^C+2n^B}$ and $\hat{z}(t) = \left[z^P(t)\ z^B(t)\right]^\top \in \mathbb{R}^{n^C+2n^B}$, respectively. The linear MLD formulation for the extended system is thus given as:

$$\begin{cases} \hat{x}(t+1) = \hat{A}\hat{x}(t) + \hat{B}_u\hat{u}(t) + \hat{B}_\delta\hat{\delta}(t) + \hat{B}_z\hat{z}(t) + \hat{D}w(t), \\ a \geq \hat{C}_x\hat{x}(t) + \hat{C}_u\hat{u}(t) + \hat{C}_\delta\hat{\delta}(t) + \hat{C}_z\hat{z}(t) + \hat{C}_w w(t), \end{cases} \tag{21}$$

where $\hat{A}$, $\hat{B}_u$, $\hat{B}_\delta$, $\hat{B}_z$, $\hat{D}$, a, $\hat{C}_x$, $\hat{C}_u$, $\hat{C}_\delta$, $\hat{C}_z$ and $\hat{C}_w$ are suitable matrices. This model is used for the modified control design in the next subsection.

3.2 Modification of the MPC

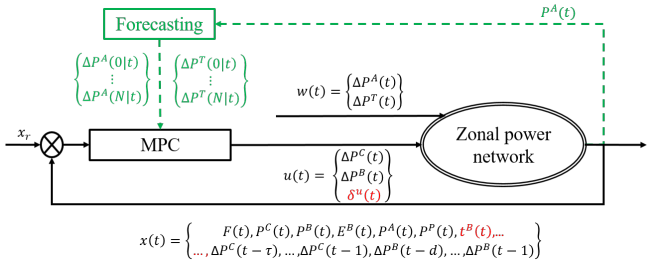

Fig. 2. Control scheme with battery specifications.

Fig. 2 describes the modified control design with respect to (11), where the additions of the variables $\delta^B(t)$ and $t^B(t)$ are highlighted in red. From (8)-(9) and (12), the constraints for the state $\hat{x}(t)$ and for the control signal $\hat{u}(t)$ are rewritten as:

$$-\overline{L} - \varepsilon(k|t) \leq C_1\hat{x}(k|t) \leq \overline{L} + \varepsilon(k|t),\ \forall k \in [d+1, N], \tag{22a}$$

$$\mathbf{0} \leq C_2\hat{x}(k|t) \leq \overline{P}^P,\ \forall k \in [\tau+1, N], \tag{22b}$$

$$\underline{C}_3\hat{u}(k-1|t) \leq C_3\hat{x}(k|t) - P^{Br} \leq \overline{C}_3\hat{u}(k-1|t), \forall k \in [1, N], \tag{22c}$$

$$\underline{E}^B \leq C_4\hat{x}(k|t) \leq \overline{E}^B,\ \forall k \in [d+1, N], \tag{22d}$$

$$u_{min} \leq C_5 \hat{u}(k|t) \leq u_{max}, \ \forall k \in [0, N-1], \quad (22e)$$

where C_1=$[\mathbf{I}_{n^L} \ \mathbf{0}]$, C_2=$[\mathbf{0}_{n^C \times n^L} \ \mathbf{I}_{n^C} \ \mathbf{0}]$, C_3=$\begin{bmatrix}\mathbf{0}_{n^B \times (n^L+n^C)} & \mathbf{I}_{n^B} & \mathbf{0}\end{bmatrix}$, $\overline{C}_3 = \begin{bmatrix}\mathbf{0}_{n^B \times (n^C+n^B)} & diag\left(\overline{P}^B_m - P^{Br}_m\right)\end{bmatrix}$, $\underline{C}_3 = \begin{bmatrix}\mathbf{0}_{n^B \times (n^C+n^B)} & diag\left(\underline{P}^B_m - P^{Br}_m\right)\end{bmatrix}$, $C_4 = \begin{bmatrix}\mathbf{0}_{n^B \times (n^L+n^C+n^B)} & \mathbf{I}_{n^B} & \mathbf{0}\end{bmatrix}$, and $C_5 = [\mathbf{I}_{n^C+n^B} \ \mathbf{0}]$. The cost function (10) is reformulated as:

$$\hat{J}(t) = \sum_{k=1}^{N} \Big[\|\hat{x}(k|t) - \hat{x_r}\|^2_{\hat{Q}} + \|\hat{u}(k-1|t)\|^2_{\hat{R}} + \|\varepsilon(k|t)\|^2_{\beta} \Big], \quad (23)$$

where $\hat{x_r} = [x_r, \mathbf{0}]^\top$, $\hat{Q} = blkdiag(Q, \mathbf{0})$, $\hat{R} = blkdiag(R, \mathbf{0})$. The modified MPC optimization problem is:

$$\mathcal{O}_2 = \underset{\{\hat{u}(0|t),\ldots,\hat{u}(N-1|t)\}}{\text{argmin}} \ \hat{J}(t) \text{ in } (23)$$
$$s.t. \ (21) \ \forall k \in [d+1, N], \ (22). \quad (24)$$

The implementation of the optimisation problem (24) includes $(n^L + (4+\tau)n^C + (5+d)n^B)N + n^L(\tau - d)$ real and $(n^C + 3n^B)N$ binary variables. The control design using this optimization problem will be validated on an industrial case study in the next section.

4. SIMULATIONS

This section presents closed-loop simulations for a sub-transmission zone composed by six nodes, seven lines, four generators and one battery. The renewable power profile is based on real data, and depicted in Iovine et al. (2021). The parameters of the model, control algorithm and simulations are presented in Table 1. The simulations are implemented in MATLAB; the control algorithms are programmed by using YALMIP in Löfberg (2004); the MPC optimization problems are solved by using CPLEX solver. Suitable values of M and γ in (5), M_1 in (16) and M_3 in (18) are chosen using the function *implies* in YALMIP, while a manual choice for M_2 in (18) is given in Table 1. The real power transmission network is emulated in these simulations through the implementation of the function *runpf* in MATPOWER toolbox for the whole French transmission network including around 6000 buses (Josz et al. (2016)). Notice that, in this network simulator, the assumptions on $\Delta P^A(t)$ and $\Delta P^T(t)$ presented in the *Estimation* block are not considered. Indeed, a scenario achieved from the historical data is used for $\Delta P^A(t)$ and the values of $\Delta P^T(t)$ are derived from the simulation with MATPOWER toolbox.

Three following simulation scenarios are implemented:

- In Scenario 1, the control designs based on the linear zone model in Iovine et al. (2021) is employed where the constraints and cost function in the MPC optimization problem are similar to $\mathcal{O}_1$. The obtained simulation results are named *linear* and represented by violet dotted curves.
- In Scenario 2, the control designs in Section 2.2 with the optimization problem $\mathcal{O}_1$ in (11) is employed. The obtained results are named *nonlinear* and represented by blue solid curves.
- In Scenario 3, the control designs in Section 3.2 with the modified optimization problem $\mathcal{O}_2$ in (24) is employed. The obtained results are named *battery spec* and represented by black dash-dotted curves.

Table 1. Parameters.

Parameter	Value
Number of nodes n^N and of lines n^L	6 and 7
Number of curtailed generators n^C	4
Number of batteries n^B	1
Line power limit L_j [MW]	45
Generators power limits $\bar{P}^G$ [MW]	$[78\ 66\ 54\ 10]^\top$
Battery power limits $[\underline{P}^B \ \bar{P}^B]$ [MW]	[-10 10]
Battery delay d [s]	5
Curtailment actuator delay τ [s]	35
Prediction horizon N	10
State weight matrix Q	$diag\{\mathbf{0}_{7\times7} \ \mathbf{I}_4 \ 10^{-3} \ \mathbf{0}_{34\times34}\}$
Input weight matrix R	$\mathbf{I}_5$
Battery availability parameters T^B_{on} [s]	35
Battery unavailability parameters T^B_{off} [s]	20
Battery power reference P^{Br} [MW]	0
Large value M_2 in (18)	1000
Relaxation weight β	10^4
Sampling time T [s]	5
Simulation time [s]	600

The maximal durations of solving the MPC optimization problem in these scenarios are 117 ms, 117 ms and 131 ms, respectively.

Fig. 3 and 4 illustrate the curtailment power and its variation, respectively, in Scenario 1 and 2. We can see that the curtailment power action takes place earlier and is greater in magnitude when considering the linear model, with respect to the nonlinear model. Hence, more energy is curtailed in the case of linear model, 1456 [MW], while only 1414 [MW] when using the nonlinear model. Even with $n^B N = 40$ additional binary variables, the maximal solving time of the optimization problem in Scenario 2 is still approximate to the one in Scenario 1. Related to the line power flow limit (22a) in scenario 2, the constraint violation is predicted at 27% of simulation iterations with the maximal value of 1.6 MW.

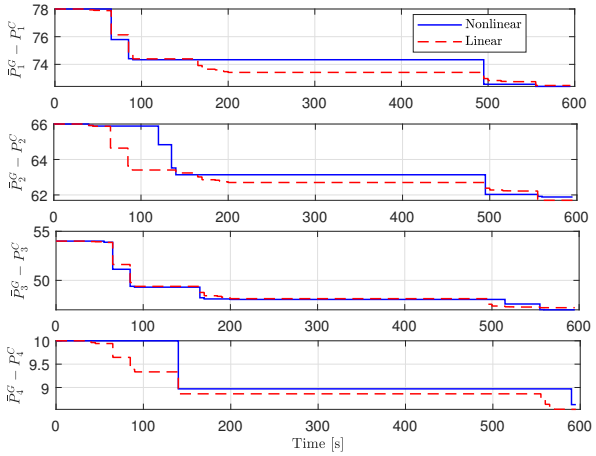

Fig. 3. Allowed produced power in Scenario 1 and 2.

Fig. 5 presents the battery power and its variation in Scenario 2 and 3. The red dash line represents the time-varying lower bound of battery power described in (12). Since the battery charging is preferred to the curtailment for dealing with surplus renewable produced power (see the weight matrix value Q in Table (1)), the battery could be expected to be maximally charged as in Scenario 2. However, this is not the case in Scenario 3 during $[65, 85]s$

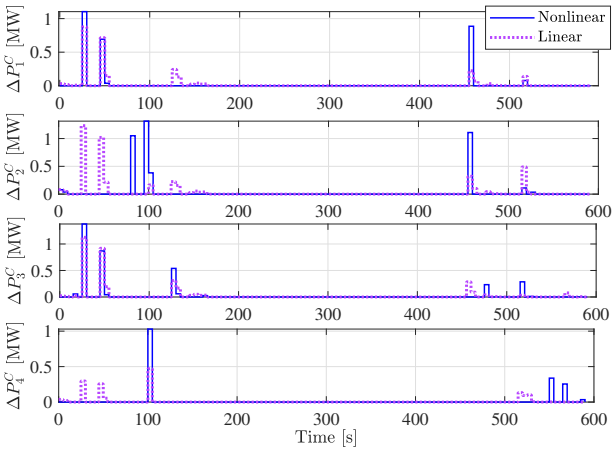

Fig. 4. Curtailment power variation in Scenario 1 and 2.

due to the difference between the real available power $P^A(t)$ and its estimation presented in Section 2.2. Indeed, during $[50, 65]s$, surplus production of renewable power are predicted in the control design thanks to its previous measurements and the forecasted value $P^A(k|t)$ described in Section 2.2. Moreover, the unavailability of the battery from $t = 85s$ is also considered in the optimization problem (24). Therefore, important amounts of renewable power curtailment are decided. Consequently, since the actually produced renewable power during $[65, 85]s$ is smaller than predicted in the past control mechanism and the curtailment action respects the delay, the maximal battery charging is not necessary. This situation is also true for the next battery availability periods. These countereffects, even if undesired, are forced by the constraints on the possibility to use the battery. However, the proposed modelling and adopted control strategy are shown to successfully manage the power congestion problem.

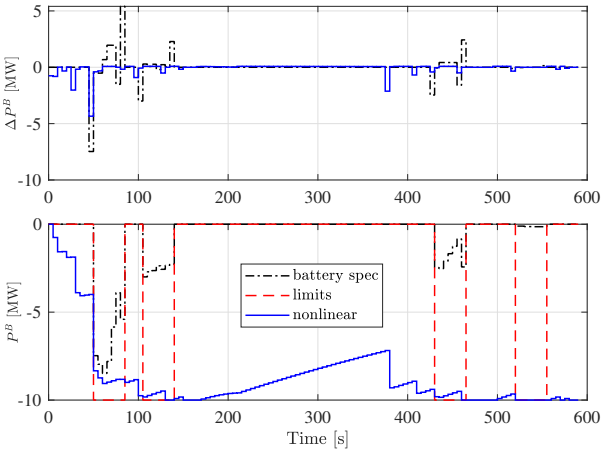

Fig. 5. Battery power and its variation in Sce. 2 and 3.

5. CONCLUSIONS

The present paper proposed two controllers for the congestion management of transmission power networks via MPC when considering nonlinearities in the modelling of produced renewable power and supplementary temporal specifications of battery availability. The nonlinear model related to the minimum operator is described as a linear Mixed Logical Dynamical (MLD) system thanks to additional logical and real variables. Hence, the integration of this linear modelling in MPC design allowed an exact consideration of the system dynamics in the optimization problem. On the other hand, to describe the battery specifications in a linear formulation, temporal and logical variables were added as system state and control signals, thus leading to an extended linear MLD model for the global system. The proposed MLD models are used in a receding horizon control approach via MPC and MILP, and have been validated through simulations on an industrial case-study of interest. The short term future work focuses on the signal temporal logic formulation for modelling the overload tolerance and battery specifications.

REFERENCES

Bemporad, A. and Morari, M. (1999). Control of systems integrating logic, dynamics, and constraints. *Automatica*, 35(3), 407–427.

Cheng, X. and Overbye, T. (2005). PTDF-based power system equivalents. *IEEE Transactions on Power Systems*, 20(4), 1868–1876.

Hoang, D.T., Olaru, S., Iovine, A., Maeght, J., Panciatici, P., and Ruiz, M. (2021). Power Congestion Management of a sub-Transmission Area Power Network using Partial Renewable Power Curtailment via MPC. In *60th IEEE Conference on Decision and Control*, 6351–6358.

Iovine, A., Hoang, D.T., Olaru, S., Maeght, J., Panciatici, P., and Ruiz, M. (2021). Modeling the partial renewable power curtailment for transmission network management. In *2021 IEEE Madrid PowerTech*, 1–6.

Josz, C., Fliscounakis, S., Maeght, J., and Panciatici, P. (2016). AC power flow data in MATPOWER and QCQP format: itesla, RTE snapshots, and PEGASE. *arXiv:1603.01533*.

Löfberg, J. (2004). Yalmip : A toolbox for modeling and optimization in matlab. In *In Proceedings of the CACSD Conference*. Taipei, Taiwan.

Meyer, B., Astic, J., Meyer, P., Sardou, F., Poumarede, C., Couturier, N., Fontaine, M., Lemaitre, C., Maeght, J., and Straub, C. (2020). Power Transmission Technologies and Solutions: The Latest Advances at RTE, the French Transmission System Operator. *IEEE Power and Energy Magazine*, 18(2), 43–52.

Monforti-Ferrario, F. and Blanco, M.P. (2021). The impact of power network congestion, its consequences and mitigation measures on air pollutants and greenhouse gases emissions. A case from Germany. *Renewable and Sustainable Energy Reviews*, 150, 111501.

Perez, A., Moreno, R., Moreira, R., Orchard, M., and Strbac, G. (2016). Effect of battery degradation on multi-service portfolios of energy storage. *IEEE Transactions on Sustainable Energy*, 7(4), 1718–1729.

Raman, V., Donzé, A., Maasoumy, M., Murray, R.M., Sangiovanni-Vincentelli, A., and Seshia, S.A. (2014). Model predictive control with signal temporal logic specifications. In *53rd IEEE Conference on Decision and Control*, 81–87.

Straub, C., Maeght, J., Pache, C., Panciatici, P., and Rajagopal, R. (2019). Congestion management within a multi-service scheduling coordination scheme for large battery storage systems. In *2019 IEEE Milan PowerTech*, 1–6.